URSI AP-RASC 2019, New Delhi, India, 09 - 15 March 2019

On the performance of the SKA mid-frequency array's reflector system and its feeds

Robert Lehmensiek* (1), and Dirk I.L. de Villiers (2)
(1) EMSS Antennas, Stellenbosch, South Africa
(2) Stellenbosch University, Stellenbosch, South Africa

Abstract

This paper compares the performance of a theoretical ideal feed to the actual designed and built feeds placed at the focus of the shaped offset Gregorian reflector antennas of the Square Kilometre Array (SKA) radio telescope. This gives an indication of how close the performance of the real feeds is to that of an ideal feed. The main metric is the receiving sensitivity and this is calculated using measured receiver temperatures.

1. Introduction

The mid-frequency array of the Square Kilometre Array (SKA) radio telescope consists of shaped offset Gregorian reflector antennas. The reflector system is in a tip-down configuration and the sub-reflector includes an extension at the bottom to shield the ground noise from the feed. The telescope's current frequency band, 350 MHz – 15.4 GHz, will be covered with six single pixel feeds that generate a single boresight beam per antenna. At the lowest frequency end is a 3:1 wide-band feed and the rest are quasi-octave band feeds. The reflector system has a mapping function that was optimized by means of a full parametric search given a set of real feeds that were the best options at the time [1].

Given this reflector system, the question may arise, how close in system performance are the present feed designs to an upper limit [2, 3]? Here the performance metric is the receiving sensitivity, which is defined as the ratio of the effective aperture area to system noise temperature (A_e/T_{sys}).

This paper compares the performance limit of an ideal feed to that of the actually built feeds in terms of receiving sensitivity given their measured receiver temperatures. Only the lower two feed frequency bands are investigated in this paper, i.e. Band 1, 350 MHz – 1050 MHz; and Band 2, 950 MHz – 1760 MHz. Band 1 is a quad-ridged flared horn [4] and Band 2 a wide flare angle axially corrugated conical horn [5].

2. Problem description

In the geometric optics (GO) limit the reflector system's mapping function $\rho(\theta_f)$ defines the relationship between the feed radiation pattern $G(\theta_f)$ and the aperture field distribution $E(\rho)$ (both axially symmetric) as follows:

$$\left|G(\theta_f)\right|^2 = \frac{V_c \left|E(\rho)\right|^2 \rho(\theta_f)\rho'(\theta_f)}{\sin\theta_f} \qquad (1),$$

where θ_f is the polar angle in the feed coordinate system, ρ is the distance from the projected aperture central axis, and V_c is a normalization constant. The apostrophe indicates the derivative with respect to θ_f.

In order to maximize the effective aperture area A_e, a uniform aperture field distribution is required, i.e. $E(\rho)=1$. Given the reflector system's mapping function the required ideal feed radiation pattern is then given in (1) over the subtended angle of the sub-reflector θ_e. For angles larger than θ_e, $G(\theta_f)$ should be zero to maximize the spillover efficiency. High edge taper values will have significant edge diffraction (mainly from the sub-reflector) and degrade the aperture efficiency performance. These effects are taken into account in the performance limit predictions below using GRASP's PO and physical theory of diffraction (PTD) technique [6].

Slightly over illuminating the sub-reflector with its extension increases the aperture efficiency. The ideal feed pattern from the mapping function is then extended past the subtended angle using linear extrapolation up to an angle θ_{ext}. Subsequently the pattern is weighted by a hybrid uniform/Gaussian function to allow the central part of the pattern to remain identical to the ideal case, while simultaneously applying a stronger taper to the pattern close to the edge. The weighting function takes the form

$$P = \begin{cases} 1, & 0 \le \theta \le \sigma_\theta \theta_e \\ \exp\left[-b_\theta \left(\dfrac{\theta - \sigma_\theta \theta_e}{\theta_e (1-\sigma_\theta)}\right)^2\right], & \sigma_\theta \theta_e \le \theta \le \theta_e \end{cases} \qquad (2),$$

where the constant b_θ controls the edge taper and σ_θ controls the extent of the central uniform power distribution. In this way a parametrized ideal feed pattern

with three parameters, namely θ_{ext}, b_θ , σ_θ , is created. This pattern is discontinuous and not realizable with a finite-sized feed. Using spherical wave expansion (SWE) we can apply a spatial filter, defined by a sphere with radius r_0 that fully encloses the feed, to the ideal radiation pattern and generate a theoretically realizable feed with a continuous feed pattern. In practice this filtering translates to limiting the number of expansion modes to N, as given by [7]

$$N = kr_0 + \max(3.6\sqrt[3]{kr_0}, 10) \quad (3),$$

where $k = 2\pi/\lambda$ is the wavenumber and λ the wavelength.

The maximum radius of the sphere enclosing the feeds r_0 was taken as 0.65 m and 0.4 m for Band 1 and Band 2 respectively, i.e. similar to the sizes of the real feeds.

Through a full parametric study of the ideal feed pattern on the SKA reflector system the upper limit of receiving sensitivity, and the associated ideal feed parameters, are determined. Note that the ideal feed parameters as optimised for aperture efficiency in [2] are different to those when optimised for receiving sensitivity and these in turn are a function of the receiver temperature.

3. Results

The noise temperatures of the feed horn and receiver were measured by hot/cold load measurements using three measurement set-ups: 1. feed pointing towards zenith and using the sky as the cold load, 2. feed placed at the focus of a MeerKAT dish (energy is then focused towards a point on the sky), and 3. using a dedicated noise test fixture (only for Band 2). For cases 1 and 2 the hot load is realized by pointing the feed into a radiation absorbent material (RAM) block at ambient physical temperature. The GSM2008 global sky model [8] was used to determine the cold load power given the simulated radiation patterns. In case 3 a carefully designed single mode transducer terminated in a cryogenically cooled attenuator and a calibrated noise source was used as a hot/cold waveguide load. In this case the noise temperature is determined of only the receiver, i.e. without the horn.

Environmental RFI is removed in cases 1 and 2 and the various measurements were averaged and approximated by a linear function. For Band 1 a 16 K temperature constant over frequency was assumed - perhaps chosen slightly optimistic. For Band 2 a realistic noise temperature that varies linearly over the frequency band from 4 K to 7.5 K is used – perhaps slightly pessimistic at the high frequency end. Note that the Band 2 receiver is cryogenically cooled and Band 1 not.

Figure 1 gives the predicted receiving sensitivities of the ideal feed and the actually built feeds and these sensitivities are compared as a ratio in percentage in Figure 2. Only the vertical polarization is shown. The sensitivity is given as the average over the tipping angles from 0° to 70°. The reduced sensitivity for lower frequencies is due to lower efficiency (due to edge diffraction) and increased sky brightness temperature. A lower receiver temperature will increase the difference between the ideal and real feed cases.

In terms of sensitivity, the current Band 2 feed antenna thus provides performance within a few percent of the maximum achievable values. For Band 1 it is slightly worse.

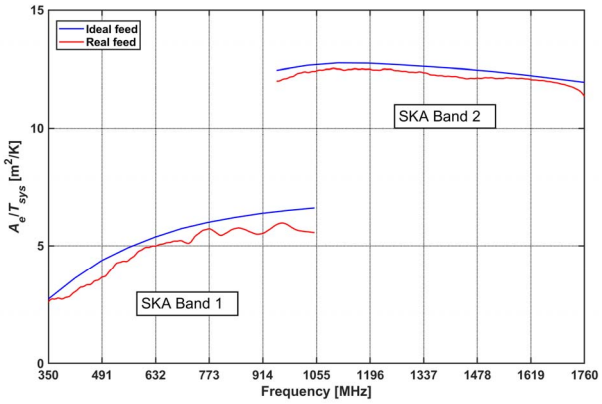

Figure 1. Receiving sensitivities averaged over tipping angles of the ideal feed and the real feeds assuming a receiver noise temperature of 16 K in Band 1 and a linear varying temperature from 4 K to 7.5 K in Band 2.

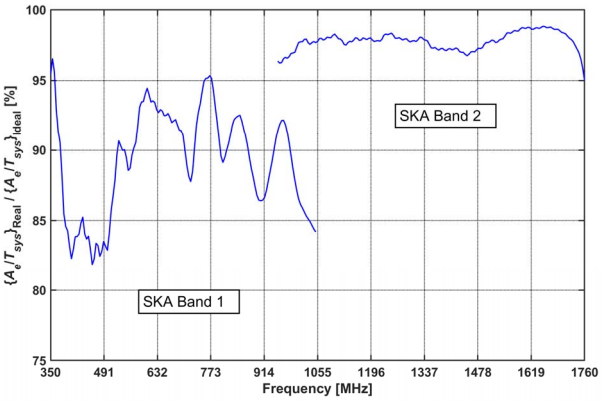

Figure 2. The ratio of the real to ideal feeds receiving sensitivities.

6. Acknowledgements

This research was supported in part by the National Research Foundation (NRF) of South Africa, and in part by the South African Radio Astronomy Observatory, which is a facility of the NRF, an agency of the Department of Science and Technology (Grant Numbers: 105717 and 75322).

7. References

1. R. Lehmensiek, I. P. Theron and D. I. L. de Villiers, "Deriving an optimum mapping function for the SKA shaped offset Gregorian reflectors," *IEEE Trans. Antennas Propag.*, **63**, 11, Nov. 2015, pp. 4658-4666.

2. R. Lehmensiek and D. I. L. de Villiers, "Aperture efficiency performance limits of the SKA reflector system," in *Proc. IEEE Int. Symp. AP & USNC/URSI Nat. Radio Sci. Meet.*, San Diego, CA, Jul. 2017, pp. 989-990.

3. R. Lehmensiek and D. I. L. de Villiers, "On the performance limits of the SKA1-mid reflector system," in *32nd URSI General Assembly and Scientific Symposium (GASS)*, Montreal, QC, Canada, Aug. 2017.

4. B. Billade, J. Flygare, M. Dahlgren, B. Wästberg and M. Pantaleev, "A wide-band feed system for SKA band 1 covering frequencies from 350 – 1050 MHz," in *Proc. 10th Eur. Conf. Antennas and Propag. (EuCAP)*, Davos, Switzerland, Apr. 2016, pp. 1-3.

5. R. Lehmensiek and I. P. Theron, "The design of the MeerKAT UHF band feed," in *Proc. 8th Eur. Conf. Antennas and Propag. (EuCAP)*, The Hague, Netherlands, Apr. 2014, pp. 880-884.

6. TICRA, GRASP10, Version 10.0.1, Copenhagen, Denmark. [Online]. Available: http://www.ticra.com.

7. F. Jensen and A. Frandsen, "On the number of modes in spherical wave expansions," in *Proc. 26th Antenna Meas. Tech. Association (AMTA)*, Stone Mountain Park, GA, Oct. 2004, pp. 489-494.

8. A. de Oliveira-Costa, M. Tegmark, B. M. Gaensler, J. Jonas, T. L. Landecker and P. Reich, "A model of diffuse Galactic radio emission from 10 MHz to 100 GHz," *Mon. Not. R. Astron. Soc.*, **388**, 1, Jul. 2008, pp. 247-260.